Tetrahedron 66 (2010) 1483–1488

Contents lists available at ScienceDirect

Tetrahedron

journal homepage: www.elsevier.com/locate/tet

Synthesis, opto-physics, and electroluminescence of cyclometalated iridium (III) complex with alkyltrifluorene picolinic acid

Yafei Wang [a], Hua Tan [a], Yu Liu [a], Chenxian Jiang [a], Zhengyong Hu [a], Meixiang Zhu [a], Lei Wang [b], Weiguo Zhu [a,*], Yong Cao [b]

[a] Key Lab of Environment-Friendly Chemistry and Application of the Ministry of Education, College of Chemistry, Xiangtan University, Xiangtan 411105, China
[b] Institute of Polymer Optoelectronic Material and Devices, South China University of Technology, Guangzhou 510640, China

ARTICLE INFO

Article history:
Received 27 September 2009
Received in revised form
24 November 2009
Accepted 1 December 2009
Available online 4 December 2009

Keywords:
OLEDs/PLEDs
Fluorene
Iridium (III)
Synthesis

ABSTRACT

To improve the opto-physics, electroluminescence, and dispersibility of iridium (III) complexes in polymer light-emitting devices, we synthesized and characterized two red-emitting heteroleptic cyclometalated iridium (III) complexes of $(Piq)_2Ir(Tfl\text{-}pic)$ and $(Piq)_2Ir(Brfl\text{-}pic)$, in which Piq is 1-phenylisoquinoline, Tfl-pic and Brfl-pic are alkyltrifluorene- and dibromoalkylfluorene-containing picolinic acid derivatives bridged with alkoxy chain, respectively. Compared to $(Piq)_2Ir(pic)$ and $(Piq)_2Ir(Brfl\text{-}pic)$, $(Piq)_2Ir(Tfl\text{-}pic)$ exhibited higher thermal stability, better dispersibility and excellent quantum efficiency. High-efficiency red emission with a maximum current efficiency of 6.28 cdA^{-1} and a maximum EL peak at 608 nm was obtained in the $(Piq)_2Ir(Tfl\text{-}pic)$-doped devices using a blend of poly(9,9-dioctylfluorene) and 2-(4-biphenyl)-5-(4-*tert* -butylphenyl)-1,3,4-oxadiazole as a host matrix.

1. Introduction

Third-row transition-metal complexes are well-known for their ability to achieve high-efficiency phosphorescence at room temperature.[1,2] In theory, this kind of cyclometalated complexes has 100% internal quantum efficiency, because they can effectively harvest both singlet and triplet excitons.[3] As a result, Ru^{II}-, Os^{II}-, Ir^{III}-, and Pt^{II}- based cyclometalated complexes have been significantly developed and exhibited wide application in organic/polymer light-emitting devices (OLEDs/PLEDs).[4–7] In these reported transition-metal complexes, iridium (III) complexes displayed best electro- phosphorescence with an external quantum efficiency as high as 27% in OLEDs and are considered to be a class of promising electrophosphorescent materials due to their non-planar configuration and short phosphorescent lifetime.[8–13]

However, there is a crucial issue of phase separation between iridium (III) complexes and host materials to influence the doped device performance. In order to overcome this issue, we once incorporated a bulky *tert*-butyl group into a cyclometalated ligand of 2-phenylpyridine and obtained a green-emitting heteroleptic iridium (III) complex with improved dispersibility and high-efficiency emission in PLEDs.[14] Some groups reported a series of high-efficiency iridium (III) complexes by introducing other bulky, rigid comphor-like alky-fluorene and dentritic architecture into cyclometalated ligands to effectively suppress the aggregation effect and improve dispersibility. Y Cao et al. reported the fluorenyl-substituted triarylamine on the cyclometalated ligand by π-conjugation to improve the performance of the devices,[15] Heeger et al. exhibited the cyclometalated with a fluorene moiety,[16] to enhance the solubility of the materials, Samuel et al. introduced the rigid moiety with alkyl-fluorene.[17] H Tian et al. made the highly efficient OLEDs by introduction rigid groups (carbazole, diphenylaniline) in the cyclometalated complexes.[18,19] However, there is few report on making iridium (III) complexes by modifying ancillary ligand. Kown et al. reported a new functioned-ancillary ligand phosphorescent dendrimer system with carbazole via a non-conjugated bridge.[20] In this paper, we reported another way to make high-efficiency red-emitting iridium (III) complexes with better dispersibility in PLEDs. As alkyltrifluorene has a non-planar configuration, excellent carrier-transporting and soluble properties, attaching a alkyl-trifluorene into the ancillary ligand of picolinic acid by a non-conjugated connection of a 1,6-hexyloxy group is expected to make its heteroleptic iridium (III) complex obtain an improved dispersing ability and high-efficiency emission in PLEDs. We designed and synthesized an ancillary ligands of picolinic acid derivative of 6-(6′-(9″-octyl-2″,7″-bi(9,9-dioctyl-fluoren-2-yl)fluoren-9″-yl)hexyloxy)picolinic acid (Tfl-picH) and its hetero-leptic iridium (III) complex of $(Piq)_2Ir(Tfl\text{-}pic)$. For comparison, an analogous picolinic acid derivative of 6-(6′-

* Corresponding author. Tel.: +86 731 58298280; fax: +86 731 58292251
E-mail address: zhuwg18@126.com (W. Zhu).

0040-4020/$ – see front matter © 2009 Elsevier Ltd. All rights reserved.
doi:10.1016/j.tet.2009.12.001

(2″,7″-dibromo-9″-octylfluoren-9″-yl)hexyloxy)picolinic acid (Brfl-picH) and its heteroleptic iridium (III) complex of $(Piq)_2Ir$(Brfl-pic) were also made in which Piq is 1-phenylisoquinoline. The synthetic route of two iridium (III) complexes is shown in Scheme 1. Their thermal and electrochemical properties, as well as optophysical were investigated. For higher thermal stability and better dispersibility, it is deserved for employing $(Piq)_2Ir$(Tfl-pic) as guest, a blend of poly(9,9-dioctylfluorene) (PFO) and 2-(4-biphenyl)-5-(4-*tert*-butylphenyl)-1,3,4-oxadiazole (PBD) as a host matrix, also we obtained red emission with a current efficiency as high as 6.28 cdA^{-1} at 9.8 V.

dioctyl-9*H*-fluorene in 78.0% yield.[22] Methyl, 6-(6′-(9″-octyl-2″,7″-bi(9,9- dioctyl fluoren-2-yl)fluoren-9′-yl)hexyloxy) picolinate (**5**) was prepared from a Suzuki Pd-catalyzed coupling reaction between boronic ester (**4**) and compound **3** in 61.0% yield.[22] Hydrolysis of compound **5** provided an ancillary ligand of Tfl-picH in 95.0% yield. The iridium (III) complexes of $(Piq)_2Ir$(Tfl-pic) and $(Piq)_2Ir$(Brfl-pic) were synthesized by two-step procedures with a chloride-bridged reaction of iridium chloride trihydrate with 1-phenylisoquinoline and a chloride cleavage of the resulting chloro-bridged dimmers $[(C\hat{}N)_2IrCl]_2$ with the ancillary ligand of Tfl-picH or Brfl-pic in over 50% yield based on the literatures.[10,23] As non-conjugated hexyloxy

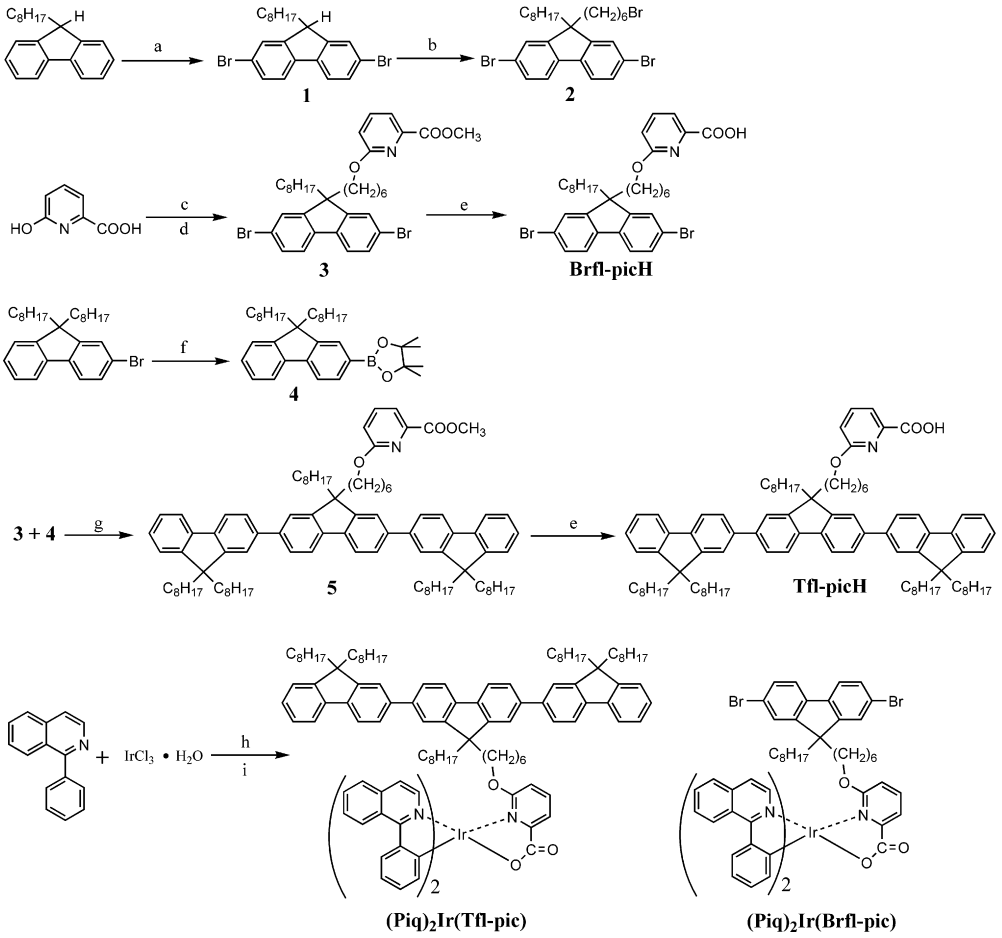

a): 0°C, Br_2, CH_2Cl_2, b): 60°C, NaOH(33%), 1,6-dibromohexane, N_2 c): reflux, CH_3OH, H_2SO_4, C_6H_6, N_2 d): reflux, acetone, K_2CO_3, KI, N_2, e): NaOH(50%), CH_3CH_2OH, THF, rt, N_2, f): 80°C, KOAc, $PdCl_2$(dppf), DMSO, N_2, g): reflux, toluene, ethanol, K_2CO_3(2M), $Pd(PPh_3)_4$, N_2, h): reflux, $IrCl_3 \bullet 3H_2O$, H_2O, 2-ethoxyethanol, N_2, i): reflux, **10** or **6**, 2-ethoxyethanol, Na_2CO_3, N_2.

Scheme 1. Synthesis route of the $(Piq)_2Ir$(Tfl-pic) and $(Piq)_2Ir$(Brfl-pic) complexes.

2. Results and discussion

2.1. Synthesis

2,7-Dibromo-9-octyl-9-(6-bromohexyl)-9*H*-fluorene (**2**) was prepared by a further nucleophilic substituted reaction of compound **1** with 1,6-dibromohexane in 71.0% yield.[21] Nucleophilic substitute of 6-hydroxypicolinic acid with compound **2** provided methyl, 6-(6′-(2″,7″-dibromo-9″-octyl-fluoren-9″-yl)hexyloxy)picolinate (**3**) in 82.3% yield. Hydrolysis of compound **3** provided an ancillary ligand of Brfl-picH in 91.8% yield. 2-(9,9-Dioctyl-9H-fluoren-2-yl)-4,4,5,5-tetramethyl-1,3,2-dioxaborolane (**4**) was synthesized by a Pd-catalyzed coupling reaction of bis(pinacolato)diboron with 2-bromo-9,9-

isolated effect, the Tfl-picH and Brfl-picH ligands have little effect on the chloride cleavage. Elemental analysis and ^1H NMR data of each of two iridium (III) complexes are consistent with the expected formula.

2.2. Optical analysis

Figure 1 shows the UV absorption spectra of these iridium (III) complexes in dichloromethane (DCM). Intense absorption band at about 352 nm and two weak absorption bands at about 405 nm and 468 nm are observed for each of two functionalized iridium (III) complexes, in which the intense high-lying absorption band is assigned to the intraligand-based π–π^* transitions, and the weak low-lying absorption band is assigned to the singlet and

triplet metal-ligand-charge-transfer (^{1}MLCT and ^{3}MLCT) transition, respectively. However, both of functionalized iridium (III) complexes presented more intense high-lying absorption band and weaker low-lying absorption bands than $(Piq)_2Ir(pic)$,[24] which have been reported by us, due to an introduction of the dibromoalkylfluorene or alkyl-trifluorene derivative into the common ancillary ligand of picolinic acid by non-conjugated connection of 1,6-hexyloxy group. In these iridium (III) complexes, $(Piq)_2Ir(Tfl\text{-}pic)$ displayed intenser high-lying absorption band. The UV absorption intensity is significantly influenced by the ancillary ligands of Tfl-picH and Brfl-picH.

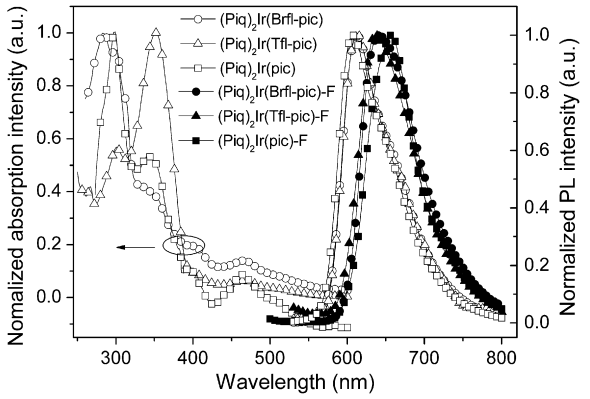

Figure 1. The normalized UV–vis and PL emission spectrum of the $(Piq)_2Ir(Tfl\text{-}pic)$, $(Piq)_2Ir(Brfl\text{-}pic)$, and $(Piq)_2Ir(pic)$complexes in DCM and neat film at room temperature.

The photoluminescence (PL) spectra of these iridium (III) complexes are also shown in Figure 1. Nearly identical PL profiles are observed for $(Piq)_2Ir(Tfl\text{-}pic)$ and $(Piq)_2Ir(Brfl\text{-}pic)$ in DCM solution or neat films. Both iridium (III) complexes displayed red emission with a peak at 612 nm in DCM solution and 638 nm in neat film, which is mainly characteristic of MLCT emission.[10] Compared to $(Piq)_2Ir(pic)$, each of functionalized iridium (III) complexes exhibited minor red-shifted emission wavelength of 6 nm in solution and displayed a blue-shifted about 16 nm in neat film. It is due to the introduction with dibromoalkylfluorene or alkyltrifluorene derivative formed the conjugated system in solution. Also, the steric alkoxy and rigid fluorene construction have an effect on the intermolecular in neat film, which induce the hypsochromic shift. Consequently, the introduction of dibromoalkylfluorene and alkyltrifluorene derivatives into iridium (III) complexes can improve their PL quantum efficiency. The photoluminescence (PL) quantum yield (Φ_{PL}) was determined to be 0.62(±10%) for $(Piq)_2Ir(Tfl\text{-}pic)$ and 0.66 (±10%) for $(Piq)_2Ir(Brfl\text{-}pic)$ in degassed DCM solution at room temperature by using $(Piq)_2Ir(acac)$ as the standard (Φ_{PL}=0.2),[25] which is three times higher than that of $(Piq)_2Ir(acac)$ and $(Piq)_2Ir(pic)$ (Table 1).

2.3. Physical properties (TGA, DSC, and AFM)

The thermal stability of these iridium (III) complexes was evaluated by TGA (heating rate of 20 °C/min) as shown in Figure S1. $(Piq)_2Ir(Tfl\text{-}pic)$ and $(Piq)_2Ir(Brfl\text{-}pic)$ exhibited a onset temperature of weight loss (T_d) of 358 °C and 311 °C, respectively, which have a better stability than the $(Piq)_2Ir(pic)$ (Table 1). Alkyltrifluorene moiety has better affected on thermal stability than dibromoalkylfluorene moiety in these iridium (III) complexes. In order to investigate their morphological property, the differential scanning calorimetry (DSC) was also measured under nitrogen atmosphere at a heating rate of 10 °C/min. As indicated in inset Figure S1, an endothermic peak centered at 121 and 122 °C was observed for $(Piq)_2Ir(Tfl\text{-}pic)$ and $(Piq)_2Ir(Brfl\text{-}pic)$, which corresponds to their melting point, respectively. The DSC curves revealed that both iridium (III) complexes are amorphous, which is particularly favored for making OLEDs because aggregation and crystallization will affect the device stability and lifetime significantly.[26] For comparison of dispersibility in polymer host matrix, the films of $(Piq)_2Ir(Tfl\text{-}pic)$ and $(Piq)_2Ir(Brfl\text{-}pic)$ doped into a blend of PBD and PVK were made, and their surface morphologies were recorded by atomic force microscopy (AFM), shown in Figure S2. The doped film with $(Piq)_2Ir(Brfl\text{-}pic)$ displayed a roughness with R_a=0.672 nm and the other doped film with $(Piq)_2Ir(Tfl\text{-}pic)$ exhibited a roughness R_a=0.242 nm, which indicates that $(Piq)_2Ir(Tfl\text{-}pic)$ has a better dispersibility than $(Piq)_2Ir(Brfl\text{-}pic)$ in the blend. The improved dispersibility of $(Piq)_2Ir(Tfl\text{-}pic)$ is attributed to the multi-octyl chains and twisted structure of the alkyltrifluorenes.

2.4. Electrochemical property

The electrochemical behavior of these cyclometalated iridium (III) complexes was studied by cyclic voltammetry using ferrocene as the internal standard and the data are listed in Table 1. Both of the iridium (III) complexes showed a sole reversible reduction wave (E^{red}) rather than a reversible oxidation wave (E^{ox}). Thus, the E^{ox} had to be estimated by the energy band gap (E_g) and E_{red} according to the formula, $E_{ox}=E_g+E_{red}$ The energy band gap was generally estimated from the low-lying absorption edge data. As a result, the highest occupied molecular orbital (HOMO) and the lowest unoccupied molecular orbital (LUMO) energy levels of these iridium (III) complexes, E_{LUMO} and E_{HOMO}, were calculated according to the following formula: $E_{LUMO}=-(E_{red}+4.34)$ and $E_{HOMO}=-(E_{ox}+4.34)$.[27] As LUMO and HOMO energies of PFO reported in literature were −2.1 eV and −5.8 eV, respectively,[28] both iridium (III) complexes here exhibited a matched energy level with the PFO host and are expected to have a carrier trap role and good electroluminescent performance in the PLEDs using PFO as a host.

2.5. Electroluminescent property

As $(Piq)_2Ir(Tfl\text{-}pic)$ presented better integrated optical and physical and electrochemical properties, it was chose as emitter

Table 1
UV–vis absorption and emission maxima, oxidation potentials, and decomposition temperature of $(Piq)_2Ir(Tfl\text{-}pic)$, $(Piq)_2Ir(Brfl\text{-}pic)$, and $(Piq)_2Ir(pic)$

Compound	Absorption[a] [nm]	Emission [nm]	E^{ox} [b] [V]	E^{red} [b] [V]	T_d [c] [°C]	Φ [%]
$(Piq)_2Ir(Tfl\text{-}pic)$	301, 352, 408, 467,	612, 672, 636 (film)	−3.12	−5.27	357	62
$(Piq)_2Ir(Brfl\text{-}pic)$	284, 353, 405, 468	612, 672, 641 (film)	−3.27	−5.25	307	66
$(Piq)_2Ir(pic)$	297, 342, 401, 464	606, 657 (film)	−2.68	−5.37	256	20

[a] As 10^{-5} M solutions in DCM.
[b] As 10^{-3} M solutions in CH_3CN containing 10^{-1} M NBu_4PF_6 as electrolyte versus ferrocene/ferrocenium.
[c] 5% weight loss.

to make devices by solution process. The device configuration is ITO/PEDOT:PSS (50 nm)/PVK (50 nm)/$(Piq)_2Ir(Tfl\text{-}pic)$+PFO–PBD (45 nm)/Ba (4 nm)Al (150 nm) (Fig. 2 inset), in which ITO/PEDOT:PSS as the anode and Ba/Al as the cathode, PVK layer is the hole transport (HT) layer, PBD behaves as both a hole-blocker and an electron-transporter. In the emitting layer, the doping weight concentration of $(Piq)_2Ir(Tfl\text{-}pic)$ varied from 1 wt% to 8 wt%, PBD weight ratio was 30% in the PFO–PBD blend.

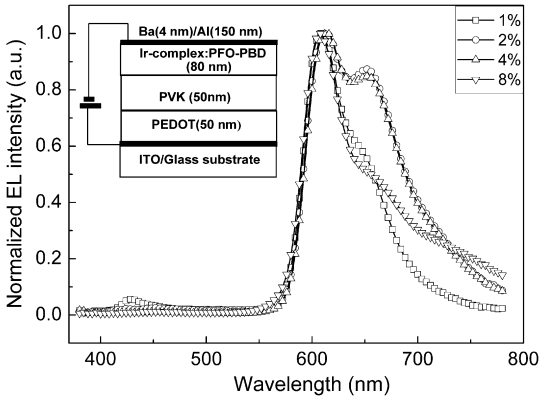

Figure 2. The structure of devices and the EL spectra of the $(Piq)_2Ir(Tfl\text{-}pic)$-doped PFO–PBD PLEDs with different concentrations.

The electroluminescence (EL) spectra of the $(Piq)_2Ir(Tfl\text{-}pic)$ doped PFO–PBD devices in the dopant concentrations from 1 wt% to 8 wt% are shown in Figure 2. Similar red-emitting EL spectra with a peak at about 608 nm and a shoulder at about 652 nm are observed in all of the devices. The fact that no emission from the host PFO+PBD appeared in the Ir (III) complex doped blend film indicated complete energy transfer from host to the Ir (III) complex expect 1 wt% doping concentration. The phenomenon with complete quenching of the host EL emission occurred at a much lower doping concentration has been attributed by some references to the charge-trapping mechanism (rather than to Förster energy transfer) followed by recombination on the chromophore (Ir complex).[29] We also note that the shoulder intensity varied with the dopant concentrations. It firstly increases with increasing dopant concentrations from 1% to 2%, and then decreases with increasing dopant concentration from 2% to 8%. The dopant concentrations have significantly an influence on the mixing single and triplet emission of MLCT.

Figure 3 exhibits the current density-voltage-luminance (J-V-L) characteristics of the $(Piq)_2Ir(Tfl\text{-}pic)$ dopant PFO–PBD devices in the doped concentrations from 1 wt% to 8 wt%. The applied voltage increases with increasing dopant concentrations at the given current density, which is attributed to the significant carrier-trap of this iridium (III) complex. The best device performance was obtained in the device at 4% dopant concentration. In order to compare to the performance difference of these devices with various dopant concentrations, the EL data of these devices were summarized in Table 2 and the current density-luminance efficiency characteristics of the devices are shown in Figure 4. The maximum luminance of 6549 cdm^{-2} and highest current efficiency of 6.28 cd/A were obtained in the device at 4% dopant concentration. The $(Piq)_2Ir(Tfl\text{-}pic)$ complex displayed better EL property than $(Piq)_2Ir(pic)$ in the PLEDs using PFO–PBD as host matrix.

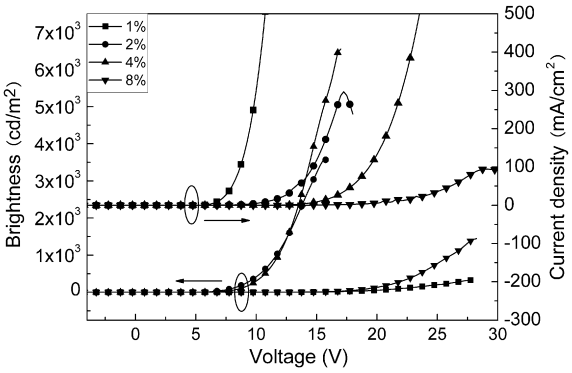

Figure 3. Current density-voltage (L-V) characteristic of the $(Piq)_2Ir(Tfl\text{-}pic)$-doped PFO–PBD PLEDs with different concentrations.

Table 2
Performance data of the $(Piq)_2Ir(Tfl\text{-}pic)$-doped PFO–PBD PLEDs with different concentrations

Host Material	Concentration [%]	Turn on Voltage[V]	λ_{max} [nm]	Luminance [cd/m^2]	η_{max} [cd/A]
PFO+PBD	1	12.25	608, 657	323	1.03
	2	5.5	612, 651	3567	3.69
	4	6.0	614, 653	6549	6.28
	8	13.0	608, 663	1455	1.53

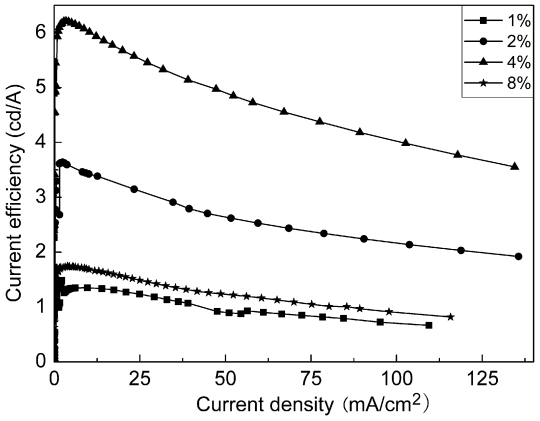

Figure 4. Current efficiency-current density characteristic of the $(Piq)_2Ir(Tfl\text{-}pic)$-doped PFO–PBD PLEDs with different concentrations.

3. Conclusion

Two red-emitting iridium (III) complexes containing dibromoalkylfluorene- and alkyltrifluorene-based picolinic acid were obtained. The iridium (III) complex with alkyl-trifluorene exhibited higher thermal stability, better dispersibility, and excellent emission quantum efficiency compared to the iridium (III) complex with dibromoalkylfluorene. High-efficiency emission with a maximum current efficiency as high as 6.2 cd/A and a maximum EL peak at 608 nm was observed in the alkyltrifluorene-containing iridium (III) complex-doped PFO–PBD devices at 4% dopant concentration. This work indicates that an introduction of alkyltrifluorene into the common picolinic acid by a non-conjugated connection of 1,6-hexyloxy is available for improving its iridium (III) complex optophysical properties and EL properties in its doped PLEDs.

4. Experimental section

4.1. Materials

All reagents were purchased from Aldrich, Acros or TCI companies. All reactions and manipulations were carried out under N_2 with the use of standard inert atmosphere and Schlenk techniques. ^{1}H NMR spectra were measured in $CDCl_3$ solution on a Bruker DPX (400 MHz) NMR spectrometer with tetramethylsilane (TMS) as the internal standard. Mass spectra (MS) were recorded on a Bruker Autoflex TOF/TOF (MALDI-TOF) instrument using dithranol as a matrix. UV–vis absorption spectroscopy was measured by Shimadzu UV-265 spectrometer at room temperature. Fluorescence spectra were recorded on RF-5301 PC (Perkin Elmer) at room temperature in dichloromethane. Cyclic voltammograms (CV) were performed with a three electrode electrochemical cell in a 0.1 M tetra(n-butyl)-ammonium hexafluorophosphate ($TBAPF_6$) solution in acetonitrile with a scan 100 mV/s at room temperature under argon. A platinum wire and a KCl saturated Hg/HgO were used as counter electrode and reference electrode, respectively. A microplatinum (ø=0.8 mm) was used as work electrode. 9-Octyl-9*H*-fluorene was prepared by a nucleophilic substituted reaction of 9*H*-fluorene with octanol based on the literature.[30,31] 2,7-Dibromo-9-octyl-9*H*-fluorene (**1**) was synthesized by a bromination of 9-octyl-9*H*-fluorene based on the procedure described by Ego.[19] 2-Bromo-9,9-dioctyl-9*H*-fluorene was synthesized based on the precedures.[32,33] The chloro-bridged dimmers of $[(C\hat{}N)_2IrCl]_2$ were gained by the chloride-bridged reaction of iridium chloride trihydrate with 1-phenylisoquinoline based on previous literatures.[10,23]

4.2. 2,7-Dibromo-9-octyl-9-(6-bromohexyl)-9*H*-fluorene (2)

A mixture of **1** (2.63 g, 6.03 mmol), 1,6-dibromohexane (14.7 g, 60.3 mmol), aqueous sodium hydroxide (33%; 20 mL), and tetrabutyl ammonium bromide (TBAB, 0.1 g) was stirred vigorously under the protection of nitrogen for 1 d at 80 °C. The mixture was cooled to room temperature and extracted with DCM (3×50 mL). The combined extracts were dried over magnesium sulfate and evaporated under reduced pressure. The excess 1,6-dibromohexane was recovered from the mixture by Kugelrohr distillation (180 °C, 0.1 mmHg). The crude product was purified by dry flash chromatography using hexane–DCM (v/v, 1:0 changing to 4:1) as eluent to give the **2** (2.57 g, 71.0%) as a colorless oil. ^{1}H NMR ($CDCl_3$, 400 MHz), δ (ppm): 7.54–7.52 (2H, d, J=8.0 Hz), 7.47–7.46 (2H, d, J=1.6 Hz), 7.45 (2H, s), 3.32–3.28 (2H, t), 1.95–1.90 (4H, t), 169–1.66 (2H, t), 1.23–1.05 (16H, m), 0.86–0.81 (5H, t).

4.3. Methyl-6-(6-(2,7-dibromo-9-octyl-9*H*-fluoren-9-yl) hexyloxy)picolinate (3)

To a stirred mixture of 6-hydroxypicolinic acid in CH_3OH and H_2SO_4 was added several drops benzene as dehydrate, the resulting mixture was refluxed for another 24 h under the protection of nitrogen. After cooled, the mixture was poured into brine and extracted with ethyl acetate (EA). The organic layer was washed with brine for three times and then dried over anhydrous Na_2SO_4. After removal of the solvent, the intermediate was gained. Then a mix of this intermediate (0.61 g, 4.0 mmol), compound **2** (2.0 g, 3.34 mmol), acetone (60 mL), K_2CO_3 (4.0 g, 40 mmol), and KI (0.5 g), the resulting mixture was refluxed for another 24 h. After cooled, the mixture was poured into brine and extracted with DCM. The organic layer was washed with brine for three times and then dried over anhydrous Na_2SO_4. After removal of the solvent, the crude product was purified by dry flash chromatography using petrol ether (PE)–EA (v/v, 10:1) as eluent to give the **5** (1.84 g, 82.3%) as a white solid. ^{1}H NMR ($CDCl_3$, 400 MHz), δ (ppm): 7.68–7.62 (2H, m), 7.52–7.50 (2H, d, J=7.92 Hz), 7.45–7.43 (2H, d, J=7.92 Hz), 4.28–4.25 (2H, t), 3.94 (3H, s), 1.94–1.89 (4H, m), 1.62–1.57 (2H, m), 1.25–1.04 (14H, m), 0.84–0.81 (3H, t), 0.59–0.58 (4H, m).

4.4. 6-(6-(2,7-Dibromo-9-octyl-9*H*-fluoren-9-yl) hexyloxy)picolinic acid (Brfl-picH)

A mixture of compound **3** (1.0 g, 1.5 mmol), NaOH (50%, 5 mL), anhydrous ethanol (5 mL), THF (10 mL) was stirred vigorously for 2 h at 60 °C, then for another 24 h at room temperature. The mixture was poured into water and extracted with DCM and the combined organic layer was dried over anhydrous magnesium sulfate. The solvent was removed by rotary evaporation and gain *Brfl-picH* (0.9 g, 91.8%) as a white solid. ^{1}H NMR ($CDCl_3$, 400 MHz), δ (ppm): 7.81 (2H, s), 7.53–7.51 (2H, d, J=7.88), 7.46–7.44 (4H, d, J=8.0), 6.98–6.96 (1H, d, J=7.44 Hz), 4.22–4.19 (2H, t), 1.96–1.89 (2H, t), 1.27–1.05 (20H, m), 0.84–0.81 (3H, t).

4.5. 2-(9,9-Dioctyl-9*H*-fluoren-2-yl)-4,4,5,5-tetramethyl-1,3,2-dioxaborolane (4)

A nitrogen-flushed three-neck round bottom flask was charged with 2-bromo-9,9-dioctyl-9*H*-fluorene (4.0 g, 8.5 mmol), bis(pinacolato)diboron (2.38 g, 9.4 mmol), potassium acetate (2.5 g, 25.5 mmol), and [1,1′-bis(diphenylphosphino)-ferrocene] dichloropalladium (0.27 mg, 0.34 mmol), complex with dichloromethane (1:1). Dimethyl sulfoxide (DMSO, 60 mL) was then added, and the mixture was bubbled with nitrogen for 15 min. After the reaction mixture was heated at 80 °C for 19 h, it was cooled to room temperature and poured into ice-water (200 mL). It was then extracted with DCM (3×20 mL) and the combined organic layer was dried over anhydrous magnesium sulfate. The solvent was removed by rotary evaporation and the residue was passed through a flash silica gel column with PE–DCM (v/v, 4:1) as the eluent to give white crystals (3.42 g, yield 78.0%). ^{1}H NMR ($CDCl_3$, 400 MHz), δ (ppm): 7.81–7.79 (2H, d, J=7.6 Hz), 7.74–7.69 (4H, m), 7.32–7.31 (2H, d, J=5.52 Hz), 2.00–1.96 (4H, t), 1.39 (12H, s), 1.20–1.02 (20H, m), 0.83–0.79 (6H, t), 0.59–0.58 (4H, m).

4.6. Methyl-6-(6-(7-(9,9-dioctyl-9*H*-fluoren-2-yl)-9,9′,9′-trioctyl-2,2′-bi(9*H*-fluoren)-9-yl)hexyl)picolinate (5)

To a mixture of compound **3** (1.0 g, 1.49 mmol), compound **4** (0.85 g, 1.64 mmol), and tetrakis(triphenylphosphine) palladium $[Pd(PPh_3)_4]$ (86 mg) was added a degassed mixture of toluene (20 mL), anhydrous ethanol (10 mL) and 2 M potassium carbonate aqueous solution (10 mL). The mixture was refluxed for 24 h under the protection of nitrogen. After cooled, the mixture was poured into water (200 mL). It was extracted with DCM (3×20 mL) and the combined organic layer was dried over anhydrous magnesium sulfate. The solvent was removed by rotary evaporation and the residue was passed through a flash silica gel column with PE–EA (v/v, 25:1) as the eluent to give an oil product. (1.16 g, yield 61.0%). ^{1}H NMR ($CDCl_3$, 400 MHz), δ (ppm): 7.86–7.76 (6H, m), 7.71–7.6 (10H, m), 7.41–7.34 (6H, m), 6.85–6.83 (1H, d, J=7.98 Hz), 4.32–4.28 (2H, t), 3.95 (3H, s), 2.08–2.05 (12H, t), 1.29–1.11 (56H, m), 0.86–0.82 (15H, t), 0.76–0.75 (12H, m).

4.7. 6-(6-(7-(9,9-Dioctyl-9*H*-fluoren-2-yl)-9,9′,9′-trioctyl-2,2′-bi(9*H*-fluoren)-9-yl)hex-yl) picolinic acid (Tfl-picH)

A mixture of compound **5** (1.0 g, 0.78 mmol), NaOH (50%, 5 mL), anhydrous ethanol (5 mL), THF (10 mL) was stirred vigorously for 2 h at 60 °C, then for another 24 h at room temperature. The mixture was poured into water and extracted with DCM and the combined organic layer was dried over anhydrous magnesium

sulfate. The solvent was removed by rotary evaporation and gain *Tfl-picH* (0.93 g, 95.0%) as a white solid. ^{1}H NMR ($CDCl_3$, 400 MHz), δ (ppm): 7.86–7.76 (6H, m), 7.71–7.6 (10H, m), 7.41–7.34 (6H, m), 6.85–6.83 (1H, d, J=7.98 Hz), 4.32–4.28 (2H, t), 2.08–2.05 (12H, t), 1.29–1.11 (56H, m), 0.86–0.82 (15H, t), 0.76–0.75 (12H, m).

4.8. Synthesis of $(Piq)_2Ir(Tfl\text{-}pic)$

To a mixture of $IrCl_3\cdot 3H_2O$ (0.3 g, 0.85 mmol) and water (5 mL) was added 1-phenylisoquinoline (0.5 g, 2.44 mmol) and 2-ethoxyethanol (15 mL). The mixture was refluxed under inert gas atmosphere for 20 h. After cooled, the colored precipitate was filtered off and was washed with water, followed by hexane. Then gain a red solid (0.42 g, 78.0%). A mixture of $[(C\text{^}N)_2IrCl]_2$ dimmers (0.2 g, 0.16 mmol), compound *Tfl-picH* (0.5 g, 0.4 mmol), and 85–90 mg of sodium carbonate were refluxed under inert gas atmosphere in 2-ethoxyethanol for 12–15 h. After cooling to room temperature, extracted with DCM and the combined organic layer was dried over anhydrous magnesium sulfate. The crude product was purified by dry flash silica gel column with DCM to gain the goal product (0.28 g, 53.0%) as a red solid. ^{1}H NMR ($CDCl_3$, 400 MHz), δ (ppm): 8.95–8.92 (1H, d, J=8.4 Hz), 8.82–8.80 (1H, d, J=9.52 Hz), 8.62–8.60 (1H, d, J=6.4 Hz), 8.12–8.10 (1H, d, J=7.6 Hz), 8.04–8.03 (1H, d, J=7.2 Hz), 7.94–7.92 (1H, d, J=7.2 Hz), 7.83–7.57 (23H, m), 7.36–7.34 (6H, d, J=7.2 Hz), 7.15–7.14 (1H, d, J=6.4 Hz), 6.89–6.86 (1H, t), 6.66–6.61 (2H, t), 6.58–6.56 (1H, d, J=8.0 Hz), 6.46–6.42 (1H, t), 6.3–6.28 (1H, d, J=8.0 Hz), 6.17–6.15 (1H, d, J=7.2 Hz), 4.27–4.26 (2H, t), 2.07–2.0 (12H, t), 1.26–1.06 (56H, m), 0.81–0.68 (27H, m). Anal. Calcd for $C_{121}H_{140}IrN_3O_3$: C 77.44, H 7.52, N 2.24. Found: C 78.94, H 7.60, N 2.34%. TOF-MS ($M+Na^+$): 1890.

4.9. Synthesis of and $(Piq)_2Ir(Brfl\text{-}pic)$

It was prepared according to the synthetic procedure of $(Piq)_2Ir(Tfl\text{-}pic)$. A red solid was obtained with a yield of 56.0%. ^{1}H NMR ($CDCl_3$, 400 MHz), 8.97–8.95 (1H, m), 8.86–8.84 (1H, d, J=9.6 Hz), 8.64–8.62 (1H, d, J=6.4 Hz), 8.14–8.12 (1H, d, J=8.4 Hz), 8.10–8.08 (1H, d, J=7.6 Hz), 7.97–7.95 (1H, d, J=7.6 Hz), 7.84–7.77 (3H, m), 7.72–7.60 (6H, m), 7.53–7.50 (2H, m), 7.46–7.42 (4H, m), 7.37–7.36 (1H, d, J=6.4 Hz), 7.20–7.18 (1H, d, J=6.4 Hz), 6.91–6.81 (1H, t), 6.70–6.62 (3H, m), 6.48–6.44 (1H, t), 6.33–6.31 (1H, d, J=7.6 Hz), 6.18–6.16 (1H, d, J=7.6 Hz), 4.28–4.25 (2H, t), 1.94–1.89 (4H, m), 1.62–1.57 (2H, m), 1.25–1.04 (14H, m), 0.84–0.81 (3H, t), 0.59–0.58 (4H, m). Anal. Calcd. For $C_{62}H_{56}Br_2IrN_3O_3$: C 59.90, H 4.54, N 3.38. Found: C 60.73, H 4.94, N 3.30%.

Acknowledgements

Financial support from the National Natural Science Foundation of China (20772101), the Science Foundation of Human Province (2009FJ2002 and 2007FJ3017) and the Postgraduate Science Foundation for Innovation in Human Province (CX2009B124 and S2008 yjscx09).

Supplementary data

TGA thermogram graph, DSC traces and atomic force microscope images for the $(Piq)_2Ir(Tfl\text{-}pic)$ and $(Piq)_2Ir(Brfl\text{-}pic)$ complexes were provided. Supplementary data associated with this article can be found in the online version at doi:10.1016/j.tet.2009.12.001.

References and notes

1. Tang, C. W.; VanSlyke, S. A.; Chen, C. H. *J. Appl. Phys.* **1989**, *65*, 3610–3616.
2. (a) Evans, R. C.; Douglas, P.; Winscom, C. J. *Coord. Chem. Rev.* **2006**, *250*, 2093–2126; (b) Thompson, M. E. *MRS Bull.* **2007**, *32*, 694–701; (c) So, F.; Krummacher, B.; Mathai, M. K.; Poplavskyy, D.; Choulis, S. A.; Choong, V. E. *J. Appl. Phys.* **2007**, *102*, 091101–091121.
3. (a) Kawamura, Y.; Goushi, K.; Brooks, J.; Brown, J. J.; Sasabe, H.; Adachi, C. *Appl. Phys. Lett.* **2005**, *86*, 071104–071106; (b) Williams, E. L.; Haavisto, K.; Li, J.; Jabbour, G. E. *Adv. Mater.* **2007**, *19*, 197–202; (c) Tong, B.; Mei, Q.; Wang, S.; Fang, Y.; Meng, Y.; Wang, B. *J. Mater. Chem.* **2008**, *18*, 1636–1639.
4. (a) Tung, Y. L.; Lee, S. W.; Chi, Y.; Chen, L. S.; Shu, C. F.; Wu, F. I.; Carty, A. J.; Chou, P. T.; Peng, S. M.; Lee, G. H. *Adv. Mater.* **2005**, *17*, 1059–1064; (b) Tung, Y. L.; Chen, L. S.; Chi, Y.; Chou, P. T.; Cheng, Y. M.; Li, E. Y.; Lee, G. H.; Shu, C. F.; Wu, F. I.; Carty, A. J. *Adv. Funct. Mater.* **2006**, *16*, 1615–1626.
5. (a) Chi, Y.; Chou, P. T. *Chem. Soc. Rev.* **2007**, *36*, 1421–1431; (b) Chou, P. T.; Chi, Y. *Eur. J. Inorg. Chem.* **2006**, 3319–3332.
6. (a) Holder, E.; Langeveld, B. M. W.; Schubert, U. S. *Adv. Mater.* **2005**, *17*, 1109–1121; (b) Flamigni, L.; Barbieri, A.; Sabatini, C.; Ventura, B.; Barigelletti, F. *Top. Curr. Chem.* **2007**, *281*, 143–203; (c) Nazeeruddin, M. K.; Gratzel, M. *Struct. Bond.* **2007**, *123*, 113–175; (d) Burn, P. L.; Lo, S.-C.; Samuel, I. D. W. *Adv. Mater.* **2007**, *19*, 1675–1688.
7. (a) Lai, S. W.; Che, C. M. *Top. Curr. Chem.* **2004**, *241*, 27–63; (b) Wong, W. Y.; He, Z.; So, S. K.; Tong, K. L.; Lin, Z. *Organometallics* **2005**, *24*, 4079–4082; (c) Chang, S.-Y.; Kavitha, J.; Li, S. W.; Hsu, C. S.; Chi, Y.; Yeh, Y. S.; Chou, P. T.; Lee, G. H.; Carty, A. J.; Tao, Y. T.; Chien, C. H. *Inorg. Chem.* **2006**, *45*, 137–146; (d) He, Z.; Wong, W. Y.; Yu, X.; Kwok, H. S.; Lin, Z. *Inorg. Chem.* **2006**, *45*, 10922–10937; (e) Williams, J. A. G.; Wilkinson, A. J.; Whittle, V. L. *Dalton Trans.* **2008**, 2081–2099; (f) Chang, S. Y.; Cheng, Y. M.; Chi, Y.; Lin, Y. C.; Jiang, C. M.; Lee, G. H.; Chou, P. T. *Dalton Trans.* **2008**, 6901–6911.
8. Su, S.; Chiba, T.; Takeda, T.; Kido, J. *Adv. Mater.* **2008**, *20*, 2125–2130.
9. Baldo, M. A.; Lamansky, S.; Burrows, P. E.; Thompson, M. E.; Forrest, S. R. *Appl. Phys. Lett.* **1999**, *75*, 4–6.
10. Lamansky, S.; Djurovich, P.; Murphy, D.; Abdel-Razzaq, F.; Lee, H. E.; Adachi, C.; Burrows, P. E.; Forrest, S. R.; Thompson, M. E. *J. Am. Chem. Soc.* **2001**, *123*, 4304–4312.
11. Lamansky, S.; Kwong, R. C.; Nugent, M.; Djurovich, P. I.; Thompson, M. E. *Org. Electron.* **2001**, *2*, 53–62.
12. Tsuzuki, T.; Shirasawa, N.; Suzuki, T.; Tokito, S. *Adv. Mater.* **2003**, *15*, 1455–1458.
13. Beeby, A.; Bettington, S.; Samuel, I. D. W.; Wang, Z. *J. Mater. Chem.* **2003**, *13*, 80–83.
14. Zhu, W. G.; Mo, Y. Q.; Yuan, M.; Wang, L.; Cao, Y. *Appl. Phys. Lett.* **2002**, *80*, 2045–2047.
15. Liang, B.; Wang, L.; Xu, Y. H.; Shi, H. H.; Cao, Y. *Adv. Funct. Mater.* **2007**, *17*, 3580–3589.
16. Gong, X.; Robinson, M. R.; Ostrowski, J. C.; Moses, D.; Bazan, G. C.; Heeger, A. J. *Adv. Mater.* **2002**, *14*, 581–585.
17. Bera, R. N.; Cumpstey, N.; Burn, P. L.; Samuel, I. W. *Adv. Funct. Mater.* **2007**, *17*, 1149–1152.
18. Xu, Z. W.; Li, Y.; Ma, X. M.; Gao, X. D.; Tian, H. *Tetrahedron* **2008**, *64*, 1860–1867.
19. Xia, Z. Y.; Xiao, X.; Sua, J. H.; Chang, C. S.; Chen, C. H.; Li, D. L.; Tian, H. *Synth. Met.* **2009**, *159*, 1782–1785.
20. Kwon, T. H.; Kim, M. K.; Kwon, J.; Shin, D. Y.; Park, S. J.; Lee, C. L.; Kim, J. J.; Hong, J. I. *Chem. Mater.* **2007**, *19*, 3673–3680.
21. Ego, C.; Marsitzky, D.; Becker, S.; Zhang, J.; Grimsdale, A. C.; Mullen, K.; MacKenzie, J. D.; Silva, C.; Friend, R. H. *J. Am. Chem. Soc.* **2003**, *125*, 437–443.
22. Pei, J.; Wang, J. L.; Cao, X. Y.; Zhou, X. H.; Zhang, W. B. *J. Am. Chem. Soc.* **2003**, *125*, 9944–9945.
23. Chen, X.; Liao, J. L.; Liang, Y.; Ahmed, M. O.; Tseng, H. E.; Chen, S. A. *J. Am. Chem. Soc.* **2003**, *125*, 636–637.
24. Huang, F. L.; Hu, Z. Y.; Wen, Z. L.; Liu, Y.; Zhu, M. X.; Zhu, W. G. *Acta Chimi. Sin.* **2008**, *66*, 2146–2150.
25. Hugo, A. B.; Chris, E. F.; Kiril, R. K.; Richard, H. F.; Charlotte, K. W. *Organometallics* **2008**, *27*, 2980–2989.
26. Sun, Y. H.; Zhu, X. H.; Chen, Z.; Zhang, Y.; Cao, Y. *J. Org. Chem.* **2006**, *71*, 6281–6284.
27. Si, Z. J.; Li, J.; Li, B.; Hong, Z. R.; Liu, S. Y.; Li, W. L. *J. Phys. Chem. C* **2008**, *112*, 3920–3925.
28. Gong, X.; Moses, D.; Heeger, A. J. *Appl. Phys. Lett.* **2003**, *83*, 183–185.
29. (a) Lane, P. A.; Palilis, L. C.; O'Brien, D. F.; Giebeler, C.; Cadby, A. J.; Lidzey, D. G.; Campbell, A. J.; Blau, W.; Bradley, D. D. C. *Phys. Rev. B: Condens. Matter Mater. Phys.* **2001**, *63*, 235206–2352113; (b) Gong, X.; Ostrowski, J. C.; Moses, D.; Bazan, G. C.; Heeger, A. J. *Adv. Funct. Mater.* **2003**, *13*, 439–444.
30. Schoen, K. L.; Becker, E. I. *J. Am. Chem. Soc.* **1955**, *77*, 6030–6031.
31. Fritz, H. E.; Peck, D. W.; Eccles, M. A.; Atkins, K. E. *J. Org. Chem.* **1965**, *30*, 2540–2542.
32. (a) Ranger, M.; Leclerc, M. *Chem. Commun.* **1997**, 1597–1598; (b) Ranger, M.; Rondeau, D.; Leclerc, M. *Macromolecules* **1997**, *30*, 7686–7691.
33. Cho, H. N.; Kim, J. K.; Kim, D. Y.; Kim, C. Y.; Song, N. W.; Kim, D. *Macromolecules* **1999**, *32*, 1476–1481.